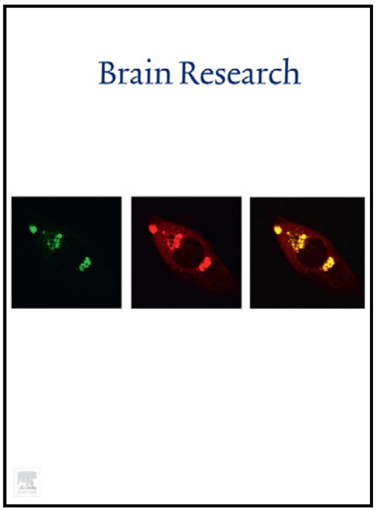

www.elsevier.com/locate/brainres

Audio-visual integration through the parallel visual pathways

Péter Kaposvári, Gerg� Csete, Anna Bognár, Péter Csibri, Eszter Tóth, Nikoletta Szabó, László Vécsei, Gyula Sáry, Zsigmond Tamás Kincses

PII: S0006-8993(15)00518-1
DOI: http://dx.doi.org/10.1016/j.brainres.2015.06.036
Reference: BRES44330

To appear in: *Brain Research*

Received date: 5 January 2015
Revised date: 20 May 2015
Accepted date: 23 June 2015

Cite this article as: Péter Kaposvári, Gerg� Csete, Anna Bognár, Péter Csibri, Eszter Tóth, Nikoletta Szabó, László Vécsei, Gyula Sáry, Zsigmond Tamás Kincses, Audio-visual integration through the parallel visual pathways, *Brain Research*, http://dx.doi.org/10.1016/j.brainres.2015.06.036

Audio-visual integration through the parallel visual pathways

Péter Kaposvári[1,*], Gergő Csete[1,2,*], Anna Bognár[1], Péter Csibri[1], Eszter Tóth[2], Nikoletta Szabó[2,3], László Vécsei[2,4], Gyula Sáry[1], Zsigmond Tamás Kincses[2,3]

[1]Department of Physiology, University of Szeged, Szeged, Hungary

[2]Department of Neurology, Albert Szent-Györgyi Clinical Centre, University of Szeged, Szeged, Hungary

[3]International Clinical Research Centre, St. Anne's University Hospital Brno, Brno, Czech Republic

[4]MTA-SZTE Neuroscience Research Group, University of Szeged

*These authors contributed equally to the experiments.

Key words: MRI, DTI, TBSS, multisensory, doubleflash

Corresponding author:
Gyula Sáry
Department of Physiology
University of Szeged
10. Dóm tér
H-6724-Szeged
HUNGARY
Email: sary.gyula@med.u-szeged.hu

Abstract

Audio-visual integration has been shown to be present in a wide range of different conditions, some of which are processed through the dorsal, and others through the ventral visual pathway. Whereas neuroimaging studies have revealed integration-related activity in the brain, there has been no imaging study of the possible role of segregated visual streams in audio-visual integration.

We set out to determine how the different visual pathways participate in this communication. We investigated how audio-visual integration can be supported through the dorsal and ventral visual pathways during the double flash illusion. Low-contrast and chromatic isoluminant stimuli were used to drive preferably the dorsal and ventral pathways, respectively. In orderto identify the anatomical substrates of the audio-visual interaction in the two conditions, the psychophysical results were correlated with the white matter integrity as measured by diffusion tensor imaging.

The psychophysiological data revealed a robust double flash illusion in both conditions. A correlation between the psychophysical results and local fractional anisotropy was found in the occipito-parietal white matter in the low-contrast condition, while a similar correlation was found in the infero-temporal white matter in the chromatic isoluminant condition. Our results indicate that both of the parallel visual pathways may play a role in the audio-visual interaction.

1. Introduction

One brief flash and two short tones presented simultaneously induce the illusion of a second flash, called the double flash illusion. Since the first description of the phenomenon (Wilson, 1987), there have been several studies looking for the possible background mechanisms. Event-related potential studies demonstrated that auditory stimuli could influence the activity of the visual cortex (Shams et al., 2001; Teder-Salejarvi et al., 2002) and an illusory flash-related gamma burst was found in primary visual areas (Bhattacharya et al., 2002; Mishra et al., 2007). Functional MRI investigations revealed illusory flash-related brain activity in the superior colliculus, the primary visual cortex and the right superior temporal sulcus (STS) (Watkins et al., 2006). These findings suggest that such interaction of the bimodal information could be based on the communication between the primary visual cortex, the STS and the primary auditory cortex (Mishra et al., 2007; Watkins et al., 2006; Watkins et al., 2007).

The higher visual cortical areas from the primary visual cortex towards the associative areas in primates are arranged to form two major information-processing streams, the dorsal and ventral pathways. These streams are traditionally regarded as the systems responsible for the representation of the 'where' and the 'what', respectively, in the visual world (Haxby et al., 1991; Ungerleider and Haxby, 1994; Wilson, 1987). The dorsal stream originates from the magnocellular pathway and is principally concerned with movement, speed of motion and location in space. The ventral stream originates from the parvocellular pathway and is responsible for the exact identification of what is seen, such as fine structure and colour. These pathways can easily be distinguished by modulating the contrast of the stimuli: stimuli with high contrast and colour are processed predominantly in the ventral stream, while stimuli with low contrast are processed in the dorsal stream (Brannan and Bodis-Wollner, 1991; Legge, 1978).

Earlier studies suggested that the double flash illusion is primarily mediated by the dorsal pathway. However, it has not yet been investigated whether the phenomenon can be evoked over both visual streams, and no systematic investigation of the involved neural structures of the dorsal and ventral streams in the illusion has yet been performed.

Electrophysiological and functional imaging studies offer a unique opportunity to investigate the contributions of various brain regions to certain functions. It is also known that function is deeply rooted in the anatomical structure, and behavioural performance is strongly influenced by the properties of the underlying brain structures. It was shown that correlation between the individual structural variability and behavioural performance can identify the neuroanatomical structures involved (Maguire et al., 2000). Furthermore, the microstructural integrity of the white matter as defined by diffusion tensor imaging is capable of revealing the coupling of structure and function (Csete et al., 2014; Johansen-Berg, 2010).

In this study we investigated the contributions of the parallel visual pathways to the double flash illusion, and aimed to identify the structural background of this processing. Using auditory stimuli to trigger the phenomenon, we set out to induce the illusion with (i) low-contrast stimuli to drive the dorsal pathway, which is sensitive to contrast and insensitive to colour information and, (ii) isoluminant stimuli to drive the ventral pathway, which is less sensitive to contrast differences. Although the distinction is not complete, this approach might be useful to investigate how additional auditory information can influence the different parts of the visual system (Kaposvari et al., 2014). We hypothesised that a better performance of an individual might relate to the higher structural integrity of the pathways involved in the processing of the stimulus. Hence, the behavioural performance in the two conditions was correlated with the diffusion MRI measured white matter microstructural integrity in order to reveal the structural background of the double flash illusion.

2. Results

2.1 Behavioural data

The subjects were tested in a double-flash paradigm, in which one or two visual stimuli following each other were presented together with a single or two consecutive tones. The measurements were repeated in two conditions: when the visual stimuli were isoluminant compared to the background (IL) (putative ventral pathway processing) and a low-contrast (LC) condition (presumably processed through the dorsal steam). According to the Signal Detection Theory, a perceptual sensitivity (d') was calculated from the correct identification of the second flashes ('hit') and from the 'false alarms'.

The paired t-test between d' values in control (one flash and two flashes without tones) and double-flash (one flash with two tones and two flashes and two tones) subconditions indicated the existence of the double flash illusion in both the LC condition ($p < 0.0003$) and the IL condition ($p < 0.0027$).The criterion revealed significant ($p<0.01$) negative bias for the double flash as compared with the control criterion in both conditions (Table 1). This shows that two tones biased the participants to report two flashes instead of one for double-flash illusions, but not the general response bias.

2.2 Correlation of behavioural data with white matter microstructural integration

In order to reveal small inter-individual variations in the white matter microstructure, which might explain the subject-to-subject differences in perceptual sensitivity we correlated the behavioral data with the diffusion parameters of the white matter.

In the IL condition, a significant positive correlation of the behavioural data (the likelihood of perceiving a double-flash illusion) and the fractional anisotropy (FA) was found in the juxtacortical infero-temporal white matter on the right and in the bilateral insulae by the Tract-Based Spatial Statistic (TBSS) analysis (Figure 1 and Table 2).

In the LC condition, a significant positive correlation was observed between FA and the likelihood of perceiving a double-flash illusion in the juxtacortical white matter of the parieto-occipital junction on the right side, the right frontal white matter under the superior frontal gyrus and bilaterally in the deep cerebellar white matter (Figure 1 and Table 3).

TBSS analysis revealed no significant correlation with any other diffusion parameters (MD, AD and RD).

2.3 Connectivity analysis

The probabilistic tractography from the infero-temporal white matter region, which revealed a high correlation with the likelihood of perceiving a double-flash illusion in the IL condition, showed tracks running along the inferior border of the temporal lobe through the inferior fronto-occipital fascicle (an association pathway connecting the occipital lobe with the frontal lobe) and the inferior longitudinal fascicle (an association pathway connecting the occipital lobe to the temporal lobe) (Figure 2).

In the LC condition, the tractography initiated from the juxtacortical parieto-occipital cluster of the TBSS analysis showed fibres along the putative arcuate fascicle, running towards the frontal lobe (Figure 2).

3. Discussion

In this study, we evoked a double-flash illusion through the dorsal and ventral stream by using low contrast and chromatic-isoluminant stimuli. Moreover, we identified correlations between the microstructure of various white matter tracks and likelihood of perceiving double-flash illusion. This correlation was found along the putative ventral and dorsal visual streams in the two conditions in which stimuli were predominantly driving the ‘what’ and ‘where’ pathways.

The visual system is traditionally subdivided to two parallel information processing pathways. The dorsal stream processes temporal information better, but its spatial resolution is inferior to that of the ventral stream, runs toward the parietal lobe. Contrary, the ventral stream, which is important for object and colour recognition, is running toward the infero-temporal structures. Importantly, in experimental protocols the two pathways can be separated by presenting low and high contrast stimuly, respectively. Finding correlation between the likelihood of perceiving double-flash illusion and white matter integrity along the ventral and dorsal streams in the two conditions driving preferentially one or the other pathway, indicate that audio-visual integration may be processed in both systems depending on the stimulus parameters.

Evidence was reported earlier of audio-visual integration occurring through the ventral stream. In a metacontrast masking paradigm, Jaekl and Harris who were able to eliminate the inhibitory effect of M-pathway-related transient activity on the P-pathway by applying a concurrent auditory stimulus, expected to increase the activity within the P-pathway (Jaekl and Harris, 2009). In the same paper, they provided further evidence by applying an orientation discrimination paradigm with an additional auditory stimulus. Here, the orientation threshold was also modulated by the concurrent auditory stimulus, which they considered to be an indication that audio-visual interactions can occur through the ventral pathway (Jaekl and Harris, 2009). Furthermore, by using chromatic stimuli, Leo et al. were able to show that, in the case of short-wavelength stimuli, processed by the parvocellular system, a significant reaction time advance can be produced by a concurrent auditory stimulus (Leo et al., 2008).

In contrast, there is also evidence that audio-visual integration may occur through the dorsal pathway. Jaekl and Soto-Faraco showed that auditory stimuli had significant effects on the contrast sensitivity in a steady, but not in a pulsed-pedestal condition, the former predominantly testing the dorsal, and the latter the ventral pathway (Jaekl and Soto-Faraco, 2010). Furthermore, an audio-visual interaction was represented at lower, but not at higher spatial frequencies, which favours the role of the M-pathway (Jaekl and Soto-Faraco, 2010). On the use of stimuli, which probably preferentially drives the M-pathway, fMRI activation differences were also detected along the M-pathway (Watkins et al., 2006; Watkins et al., 2007).

The results listed above are seemingly contradictory, though our results relating to a double-flash illusion with low contrast and with chromatic-isoluminant stimuli suggest that audio-visual integration can be evoked through both the dorsal and the ventral stream.

It is important to note that no stimulus is processed exclusively through the ventral or the dorsal pathway; the stimuli in our investigation were designed to drive preferentially the magno- or the parvocellular pathways (Kaposvari et al., 2014).

Further support of audio-visual integration taking place through both the ventral and dorsal pathways comes from the results of the DTI analysis. The likelihood of the perception of illusion in the low-contrast condition correlated with the white matter integrity of the parieto-occipital junction and the frontal white matter. Not only is the parieto-occipital region in the close vicinity of the dorsal pathway cortical regions, but its connectivity pattern resembles the dorsal pathway (Haxby et al., 1991; Ungerleider and Haxby, 1994).

Similarly, the correlation of behavioural measures with tissue integrity in the infero-temporal white matter in the case of the chromatic-isoluminant condition strongly supports the possible involvement of the ventral pathway in the audio-visual integration.

Interestingly, the correlations between the probability of double-flash illusion and the white matter integrity were lateralised;, however it has to be noted that there were correlations found on the other side also, but they were just below the threshold. Nevertheless, having lateralised results are not surprising: several studies showed asymmetric function and structure in the visual system (Antal et al., 2004; Dreessen de Gervai et al., 2014).

We also found in the literature significant correlations between structure and function in non-visual pathways. Electrophysiology and fMRI investigation showed that the insula is participating in multimodal integration (Calvert et al., 2001) and recently it was demonstrated that isochronous timing in an audiovisual task has a positive influence on insular activity (Marchant and Driver, 2013). Also several researches pointed out the importance of cerebellum in audio-visual integration (Pfordresher et al., 2014; Proverbio et al., 2014).

White matter integrity and structural connectivity were recently of interest as concerns the determination of the connection between structure and function. The variation of the connectivity profile of certain regions can predict a variation in function (Behrens et al., 2006; Johansen-Berg et al., 2004; Klein et al., 2007; Saygin et al., 2012). Local diffusion features of the white matter supported to be related to the behavioural performance (Csete et al., 2014; Johansen-Berg, 2010). A higher FA in the corpus callosum was related to a better bimanual coordination (Johansen-Berg et al., 2007). A training-induced FA increase has been detected in the intraparietal sulcus (Scholz et al., 2009). It has also been shown that a greater BOLD response in the visual cortex correlates with a higher FA in the optic radiation (Toosy et al., 2004). Neuroimaging and histological studies have been combined recently that demonstrated that spatial learning and motor learning result in locally enhanced myelination (Blumenfeld-Katzir et al., 2011; Sampaio-Baptista et al., 2013), which is reflected in enhanced FA in the diffusion MRI.

The relationships between these white matter diffusion properties and histological properties are not yet clear, but nerve diameter and myelination that relate to the microstructure measurable with DTI can also relate to the conduction velocity and dispersion of the neuronal signal (Hodgkin and Huxley, 1952). As regarding the functional significance of the diffusion-measured microstructure, recently it was shown that the FA of the white matter pathway neurophysiology measured functional connectivity of the connected regions is correlated (Boorman et al., 2007; Neubert et al., 2010).

4. Experimental Procedure

4. Subjects

Sixteen healthy subjects (10 females; mean age of 27.4 years) were enrolled in the study. None of them suffered from any neurological or psychiatric diseases. All of them had normal or corrected-to-normal (20/20) visual acuity and good colour vision. The study was approved by the ethical committee of the University of Szeged (Ref. no.: 87/2009) and all study participants gave their written informed consent in accordance with the Declaration of Helsinki.

4.2 Behavioural test

The subjects sat in a sound-attenuated dark room with their heads resting on a chin and forehead support. Their eyes were 57 cm away from the screen (ViewSonic monitor, 21" diameter, 800 x 600, 60.0 Hz) and the speakers. The two computer speakers were positioned symmetrically, on each side of the monitor, at 25˚ from the fixation point. The subjects had to fix their gaze on a black fixation dot at the middle of the monitor. A disc subtending a visual angle of 1.5˚ was displayed in a peripheral position at 9.25 eccentricity below the fixation point, as a visual stimulus (Watkins et al., 2007).

Two conditions were investigated: an isoluminant (IL) condition, where a red disc was presented on a green background (8.9 cd/m^2), and a low-contrast (LC) condition, where we used a light-grey disc (9.7 cd/m^2, contrast 9%) on a darker grey background (8.9 cd/m^2). The conditions were presented in a semi-random sequence.

The conditions contained 6 subconditions: 6 variations of flashes (one flash, one flash with one tone, one flash with two tones, two flashes, two flashes with one tone, and two flashes with two tones). One subcondition consisted of 40 repetitions of the trial, and thus one block contained 240 semi-random-presented trials.

The presentation of the trial started with the condition-specific green background in the IL condition and with the grey background in the LC condition. After 200 ms one or two discs were presented for 17 ms on this background, without or with one or two tones, according to the given condition. The stimulus onset asynchrony (SOA) between two flashes was 85 ms. The duration of the tones (3.5 kHz, 70 dBSPL) was 10 ms and was presented at the same time as the first flash. The SOA between the two tones was 85 ms. The previously mentioned experiments used auditory and visual stimuli slightly shifted in time, but as reported, the two designs with simultaneously presented or shifted stimuli resulted in only slight differences (Watkins et al., 2006). After the presentations of the flashes and tones, the subject had to decide whether one or two discs were displayed, independently of the tones, and press the left (one flash) or right arrow (two flashes) button on the keyboard with the dominant hand. After the subject had pressed a key, the grey background (8.9 cd/m^2) appeared for the inter-trial interval of 1000 ms. Feedback concerning the correctness or not of the responses was not provided.

4.3 Analysis of behavioural data

Signal detection theory was used to analyse the behavioural results. With this method, the sensitivity of the subjects towards the visual stimuli could be described. The aim was to verify that the illusions were caused by changes in perceptual sensitivity, but not by the general response bias. The sensitivity is expressed as

$d' = z(H) - z(F)$,

where d' is the sensitivity, and z is the inverse of the normal cumulative distribution. In one block, we calculated three d' values for two subconditions. The correct identification of the second flash was accepted as a 'hit' (H); if the subject reported one flash instead of two, it was recorded as a 'miss'. When one flash was reported as two, we accepted it as a 'false alarm' (F) and the correct identification of one flash was accepted as a 'correct rejection'. To calculate the *d*’ value for the control, we used the two subconditions without tones (one flash and two flashes). For double flashes, we used the two subconditions with two tones (one flash with two tones and two flashes with two tones). To examine the power of the illusions, we compared the control d' value with that for fusion or the double flash by the paired t-test (Watkins et al., 2006). A criterion (C) was calculated to indicate the response bias via the expression (MacMillan and Creelman, 2005):

$C=-[z(pH)+z(pF)]/2$,

A positive value of C indicates the bias when the subjects rather report one flash, while a negative value indicates when they rather report two flashes.

4.4 Data acquisition

Neuroimaging data acquisitions were carried out on a 1.5 T GE Signa Excite HDxt MR Scanner (GE Healthcare, Chalfont St. Giles, UK). Three-dimensional spoiled gradient echo images (FSPGR: echo time [TE]: 4.1 ms; repetition time [TR]: 10.276 ms; matrix: 256 * 256; field of view [FOV]: 25cm * 25cm; flip angel: 15 degree; in-plane resolution: 1*1 mm^2; slice thickness: 1 mm) and 60 directions diffusion-weighted images with 6 non-diffusion-weighted reference volume (TE: 93.8 ms; TR: 16,000 ms; matrix: 96*96; FOV: 23*23 cm^2; flip angle: 90 degree; in-plane resolution: 2.4*2.4 mm^2; slice thickness: 2.4 mm; b:1000 s/m2; number of excitations [NEX]: 2; array spatial sensitivity encoding technique [ASSET]) were acquired for all subjects.

4.5 Data analysis

Diffusion data were corrected for eddy currents and movements artefacts by twelve degrees of freedom affine linear registration to the first non-diffusion-weighted reference image. Diffusion tensors at each voxel were fitted by an algorithm included in FMRIB's Diffusion Toolbox (FDT) of FSL (v.4.0)(Smith et al., 2004). Fractional anisotropy (FA), mean (MD), axial (AD) and radial diffusivity (RD) was computed for the whole brain. In order to reduce the possible errors arising from misalignment of the images, we used the Tract Based Spatial

Statistics (TBSS) method (Smith et al., 2007). For all subjects, the FA images were aligned into a common space, using the non-linear registration tool, FNIRT, which uses a b-spline representation of the registration warp field. The mean FA image was created and then thresholded at FA=0.2, deriving a mean FA skeleton representing the centres of all tracts common to the group. The aligned FA data for eachsubjects were then projected onto this skeleton and the resulting data were fed into voxel-wise cross-subject statistics. Modelling and inference with the standard general linear model design set-up was accomplished by using permutation-based cluster analysis (n=5000) as implemented in the FSL software package (Nichols and Holmes, 2002). The design encoded for the differences of the d' value of the double-flash and the control d' in two conditions (isoluminant and low-contrast) from psychophysical measurements. Statistical images were thresholded by threshold free cluster enhancement (Smith and Nichols, 2009). Since our task was a relatively low level perceptual task, it would have been over-conservative to correct for multiple correlations based on the total number of voxels. Hence, we used the non-corrected stats thresholded at a 1% significance level. Only clusters larger than 5 voxels were considered for discussion. The same analysis for MD, AD and RD was repeated by projecting the various diffusion parameters to the FA skeleton.

The connectivity of the regions, which showed significant correlation with the behavioural data, was defined by the probabilistic tractography (FDT, part of FSL: www.fmrib.ox.ac.uk/fsl/fdt). A multifibre diffusion model was fitted that estimates the probability distribution in the direction of 1 or more fibre populations at each voxel (Behrens et al., 2007). Probabilistic tractography was then performed on any brain voxel by tracing streamline samples through these probabilistic distributions in the fibre direction. For tractography, we generated 5000 streamline samples from each seed voxel to build up a connectivity distribution. The number of these samples passing through each brain voxel is interpreted as proportional to the probability of the connection to the seed voxel. By fitting a multifibre model to our diffusion data, we were able to trace pathways through regions of fibre crossing (Behrens et al., 2007). The seed masks were binary cluster-masks of the TBSS analysis.

Acknowledgements

This study was supported by the "Neuroscience Research Group of the Hungarian Academy of Sciences and University of Szeged", project FNUSA-ICRC (no. CZ.1.05/1.1.00/02.0123) from the European Regional Development Fund, the National Brain Research Program (Grant No. KTIA_13_NAP-A-II/20.)and an OTKA [PD 104715] grant. The publication is supported by the European Union and co-funded by the European Social Fund. (Project title: “Telemedicine-focused research activities in the field of Mathematics, Informatics and Medical sciences” Project number: TÁMOP-4.2.2.A-11/1/KONV-2012-0073). This research was supported by the European Union and the State of Hungary, co-financed by the European Social Found in the framework of TÁMOP 4.2.4.A/2-11-1-2012-0001 ‘National Excellence Program’. A. Bognár, P. Csibri and Gy. Sáry were supported by OTKA K83671. MR imaging was carried out by Euromedic Diagnostic Ltd, Szeged.

References

Antal, A., Nitsche, M.A., Kincses, T.Z., Lampe, C., Paulus, W., 2004. No correlation between moving phosphene and motor thresholds: a transcranial magnetic stimulation study. Neuroreport. 15**,** 297-302.

Behrens, T.E., Jenkinson, M., Robson, M.D., Smith, S.M., Johansen-Berg, H., 2006. A consistent relationship between local white matter architecture and functional specialisation in medial frontal cortex. Neuroimage. 30**,** 220-7.

Behrens, T.E., Berg, H.J., Jbabdi, S., Rushworth, M.F., Woolrich, M.W., 2007. Probabilistic diffusion tractography with multiple fibre orientations: What can we gain? Neuroimage. 34**,** 144-55.

Bhattacharya, J., Shams, L., Shimojo, S., 2002. Sound-induced illusory flash perception: role of gamma band responses. Neuroreport. 13**,** 1727-30.

Blumenfeld-Katzir, T., Pasternak, O., Dagan, M., Assaf, Y., 2011. Diffusion MRI of structural brain plasticity induced by a learning and memory task. PLoS One. 6**,** e20678.

Boorman, E.D., O'Shea, J., Sebastian, C., Rushworth, M.F., Johansen-Berg, H., 2007. Individual differences in white-matter microstructure reflect variation in functional connectivity during choice. Curr Biol. 17**,** 1426-31.

Brannan, J.R., Bodis-Wollner, I., 1991. Evidence for two systems mediating perceived contrast. Vis Neurosci. 6**,** 587-92.

Calvert, G.A., Hansen, P.C., Iversen, S.D., Brammer, M.J., 2001. Detection of audio-visual integration sites in humans by application of electrophysiological criteria to the BOLD effect. Neuroimage. 14**,** 427-438.

Csete, G., Szabo, N., Rokszin, A., Toth, E., Braunitzer, G., Benedek, G., Vecsei, L., Kincses, Z.T., 2014. An investigation of the white matter microstructure in motion detection using diffusion MRI. Brain Res. 1570**,** 35-42.

Dreessen de Gervai, P., Sboto-Frankenstein, U.N., Bolster, R.B., Thind, S., Gruwel, M.L., Smith, S.D., Tomanek, B., 2014. Tractography of Meyer's Loop asymmetries. Epilepsy Res. 108**,** 872-82.

Haxby, J.V., Grady, C.L., Horwitz, B., Ungerleider, L.G., Mishkin, M., Carson, R.E., Herscovitch, P., Schapiro, M.B., Rapoport, S.I., 1991. Dissociation of object and spatial visual processing pathways in human extrastriate cortex. Proc Natl Acad Sci U S A. 88**,** 1621-5.

Hodgkin, A.L., Huxley, A.F., 1952. Propagation of electrical signals along giant nerve fibers. Proc R Soc Lond B Biol Sci. 140**,** 177-83.

Jaekl, P.M., Harris, L.R., 2009. Sounds can affect visual perception mediated primarily by the parvocellular pathway. Vis Neurosci. 26**,** 477-86.

Jaekl, P.M., Soto-Faraco, S., 2010. Audiovisual contrast enhancement is articulated primarily via the M-pathway. Brain Res. 1366**,** 85-92.

Johansen-Berg, H., Behrens, T.E., Robson, M.D., Drobnjak, I., Rushworth, M.F., Brady, J.M., Smith, S.M., Higham, D.J., Matthews, P.M., 2004. Changes in connectivity profiles define functionally distinct regions in human medial frontal cortex. Proc Natl Acad Sci U S A. 101**,** 13335-40.

Johansen-Berg, H., Della-Maggiore, V., Behrens, T.E., Smith, S.M., Paus, T., 2007. Integrity of white matter in the corpus callosum correlates with bimanual co-ordination skills. Neuroimage. 36 Suppl 2**,** T16-21.

Johansen-Berg, H., 2010. Behavioural relevance of variation in white matter microstructure. Curr Opin Neurol. 23**,** 351-8.

Kaposvari, P., Bognar, A., Csibri, P., Utassy, G., Sary, G., 2014. Fusion and fission in the visual pathways. Physiol Res.

Klein, J.C., Behrens, T.E., Robson, M.D., Mackay, C.E., Higham, D.J., Johansen-Berg, H., 2007. Connectivity-based parcellation of human cortex using diffusion MRI: Establishing reproducibility, validity and observer independence in BA 44/45 and SMA/pre-SMA. Neuroimage. 34**,** 204-11.

Legge, G.E., 1978. Sustained and transient mechanisms in human vision: temporal and spatial properties. Vision Res. 18**,** 69-81.

Leo, F., Bertini, C., di Pellegrino, G., Ladavas, E., 2008. Multisensory integration for orienting responses in humans requires the activation of the superior colliculus. Exp Brain Res. 186**,** 67-77.

MacMillan, N., Creelman, C., 2005. Detection Theory: A User's Guide Routledge. Vol., Psychology Press.

Maguire, E.A., Gadian, D.G., Johnsrude, I.S., Good, C.D., Ashburner, J., Frackowiak, R.S., Frith, C.D., 2000. Navigation-related structural change in the hippocampi of taxi drivers. Proc Natl Acad Sci U S A. 97**,** 4398-403.

Marchant, J.L., Driver, J., 2013. Visual and audiovisual effects of isochronous timing on visual perception and brain activity. Cereb Cortex. 23**,** 1290-8.

Mishra, J., Martinez, A., Sejnowski, T.J., Hillyard, S.A., 2007. Early cross-modal interactions in auditory and visual cortex underlie a sound-induced visual illusion. J Neurosci. 27**,** 4120-31.

Neubert, F.X., Mars, R.B., Buch, E.R., Olivier, E., Rushworth, M.F., 2010. Cortical and subcortical interactions during action reprogramming and their related white matter pathways. Proc Natl Acad Sci U S A. 107**,** 13240-5.

Nichols, T.E., Holmes, A.P., 2002. Nonparametric permutation tests for functional neuroimaging: a primer with examples. Hum Brain Mapp. 15**,** 1-25.

Pfordresher, P.Q., Mantell, J.T., Brown, S., Zivadinov, R., Cox, J.L., 2014. Brain responses to altered auditory feedback during musical keyboard production: an fMRI study. Brain Res. 1556**,** 28-37.

Proverbio, A.M., Calbi, M., Manfredi, M., Zani, A., 2014. Audio-visuomotor processing in the musician's brain: an ERP study on professional violinists and clarinetists. Sci Rep. 4**,** 5866.

Sampaio-Baptista, C., Khrapitchev, A.A., Foxley, S., Schlagheck, T., Scholz, J., Jbabdi, S., DeLuca, G.C., Miller, K.L., Taylor, A., Thomas, N., Kleim, J., Sibson, N.R., Bannerman, D., Johansen-Berg, H., 2013. Motor skill learning induces changes in white matter microstructure and myelination. J Neurosci. 33**,** 19499-503.

Saygin, Z.M., Osher, D.E., Koldewyn, K., Reynolds, G., Gabrieli, J.D., Saxe, R.R., 2012. Anatomical connectivity patterns predict face selectivity in the fusiform gyrus. Nat Neurosci. 15**,** 321-7.

Scholz, J., Klein, M.C., Behrens, T.E., Johansen-Berg, H., 2009. Training induces changes in white-matter architecture. Nat Neurosci. 12**,** 1370-1.

Shams, L., Kamitani, Y., Thompson, S., Shimojo, S., 2001. Sound alters visual evoked potentials in humans. Neuroreport. 12**,** 3849-52.

Smith, S.M., Jenkinson, M., Woolrich, M.W., Beckmann, C.F., Behrens, T.E., Johansen-Berg, H., Bannister, P.R., De Luca, M., Drobnjak, I., Flitney, D.E., Niazy, R.K., Saunders, J., Vickers, J., Zhang, Y., De Stefano, N., Brady, J.M., Matthews, P.M., 2004. Advances in functional and structural MR image analysis and implementation as FSL. Neuroimage. 23 Suppl 1**,** S208-19.

Smith, S.M., Johansen-Berg, H., Jenkinson, M., Rueckert, D., Nichols, T.E., Miller, K.L., Robson, M.D., Jones, D.K., Klein, J.C., Bartsch, A.J., Behrens, T.E., 2007. Acquisition and voxelwise analysis of multi-subject diffusion data with tract-based spatial statistics. Nat Protoc. 2, 499-503.

Smith, S.M., Nichols, T.E., 2009. Threshold-free cluster enhancement: addressing problems of smoothing, threshold dependence and localisation in cluster inference. Neuroimage. 44, 83-98.

Teder-Salejarvi, W.A., McDonald, J.J., Di Russo, F., Hillyard, S.A., 2002. An analysis of audio-visual crossmodal integration by means of event-related potential (ERP) recordings. Brain Res Cogn Brain Res. 14, 106-14.

Toosy, A.T., Ciccarelli, O., Parker, G.J., Wheeler-Kingshott, C.A., Miller, D.H., Thompson, A.J., 2004. Characterizing function-structure relationships in the human visual system with functional MRI and diffusion tensor imaging. Neuroimage. 21, 1452-63.

Ungerleider, L.G., Haxby, J.V., 1994. 'What' and 'where' in the human brain. Curr Opin Neurobiol. 4, 157-65.

Watkins, S., Shams, L., Tanaka, S., Haynes, J.D., Rees, G., 2006. Sound alters activity in human V1 in association with illusory visual perception. Neuroimage. 31, 1247-56.

Watkins, S., Shams, L., Josephs, O., Rees, G., 2007. Activity in human V1 follows multisensory perception. Neuroimage. 37, 572-8.

Wilson, J.T., 1987. Interaction of simultaneous visual events. Perception. 16, 375-83.

Table legends

Table 1. The mean and standard error (SEM) of the *d*' and criterion values in the behavioural tests. Please note that since the values of "Hit" and "False alarm" were rounded, the *d'* values in the table above might deviate from the correct mathematical value.

Table 2. Anatomical localization of correlations of FA with the likelihood of perceiving a double-flash illusion in the isoluminant condition. Coordinates represent standard space coordinates in the FMRIB58_FA template.

Table 3. Anatomical localization of correlations of FA with the likelihood of perceiving a double-flash illusion in thelow-contrast condition. Coordinates represent standard space coordinates in the FMRIB58_FA template.

Figure legends

Figure 1. Correlation of FA with a higher likelihood of perceiving a double-flash illusion. White matter microstructure as measured by FA, showed correlation with the perceptual sensitivity to double flash illusion in the isoluminant (upper row) and low-contrast condition (lower row). The identified white matter regions overlap with the ventral and dorsal visual pathways respectively. Images are overlaid on the FMRIB58_FA standard image. The mean FA skeleton, thresholded at 0.2, is depicted in green shades. Significant clusters are indicated in red for the isoluminant and in blue for the low-contrast condition. A thickened version of the significant cluster is used to facilitate visualization.

Figure 2. Connectivity of clusters showing the correlation between FA and behavioural data in theisoluminant (red) and low-contrast (blue) conditions. The white matter fibres identified by the tractography correspond to the ventral and dorsal visual pathways in the isoluminant and low-contrast conditions respectively. The binary cluster masks were used as seed mask for each subject. Five thousand streamline samples from each seed voxel were drawn to build up a connectivity distribution that was thresholded for 1000 particles for each subject and binarized. Population connectivity maps were derived for controls by adding these masks together and thresholding at four (Pathways passing through the given voxel in at least four subjects).

Conditions		*d*' mean	±SEM	*C* mean	±SEM	Hit mean	±SEM	False alarm mean	±SEM
Isoluminant	control	3.592	0.211	0.087	0.140	0.9084	0.0229	0.0813	0.0253
	double flash	1.721	0.244	-1.605	0.180	0.9750	0.0108	0.6667	0.0761
Low contrast	control	3.461	0.216	-0.057	0.130	0.9229	0.0210	0.0917	0.0244
	double flash	1.917	0.270	-1.604	0.166	0.9729	0.0115	0.6521	0.0811

	p<	No. ofvoxels	X (mm)	Y (mm)	Z (mm)
Right insular WM	0.001	56	36	12	-14
Right infero-temporal WM	0.001	33	45	-60	-8
Left insular WM	0.001	10	-32	21	0

	$p<$	No.of voxels	X (mm)	Y (mm)	Z (mm)
Cerebellar WM	0.001	582	-17	-65	-33
Right parieto-occipital junction	0.001	53	52	-51	9
Right fronto-polar WM	0.001	10	22	56	7
Right superior frontal WM	0.005	4	17	21	51

A robust double flash illusion was found using both magno and parvo optimalized visual stimuli.

DTI data show correlation between psychophysical results and local fractional anisotropy.

The low contrast condition revealed a positive correlation between the local fractional anisotropy and the occipito-parietal white matter.

In the isoluminant condition similar correlation was found in the infero-temporal white matter.

Tractography originating from these areas matches the dorsal and ventral visual pathways.

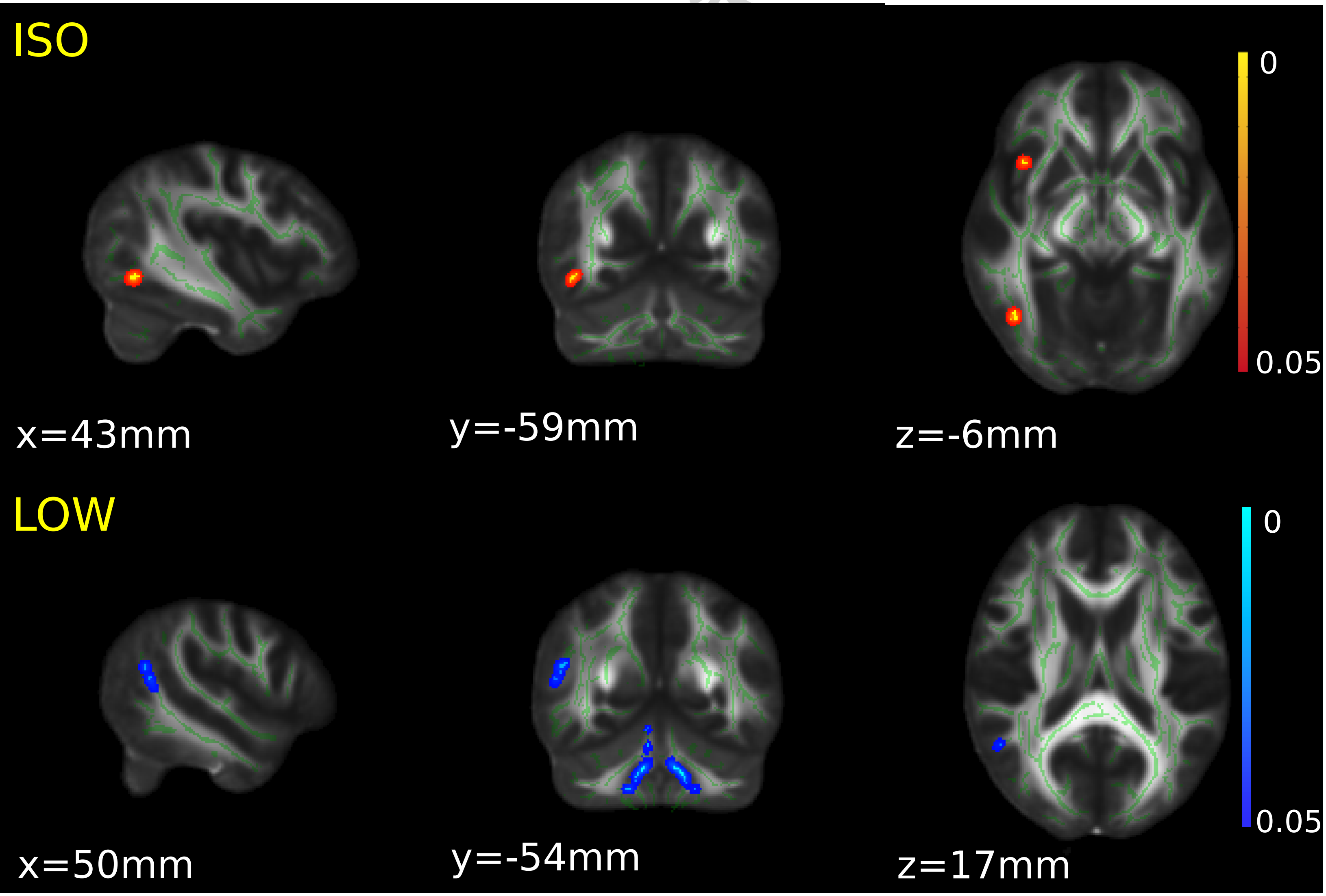
ISO
0
0.05
x=43mm
y=-59mm
z=-6mm
LOW
0
0.05
x=50mm
y=-54mm
z=17mm

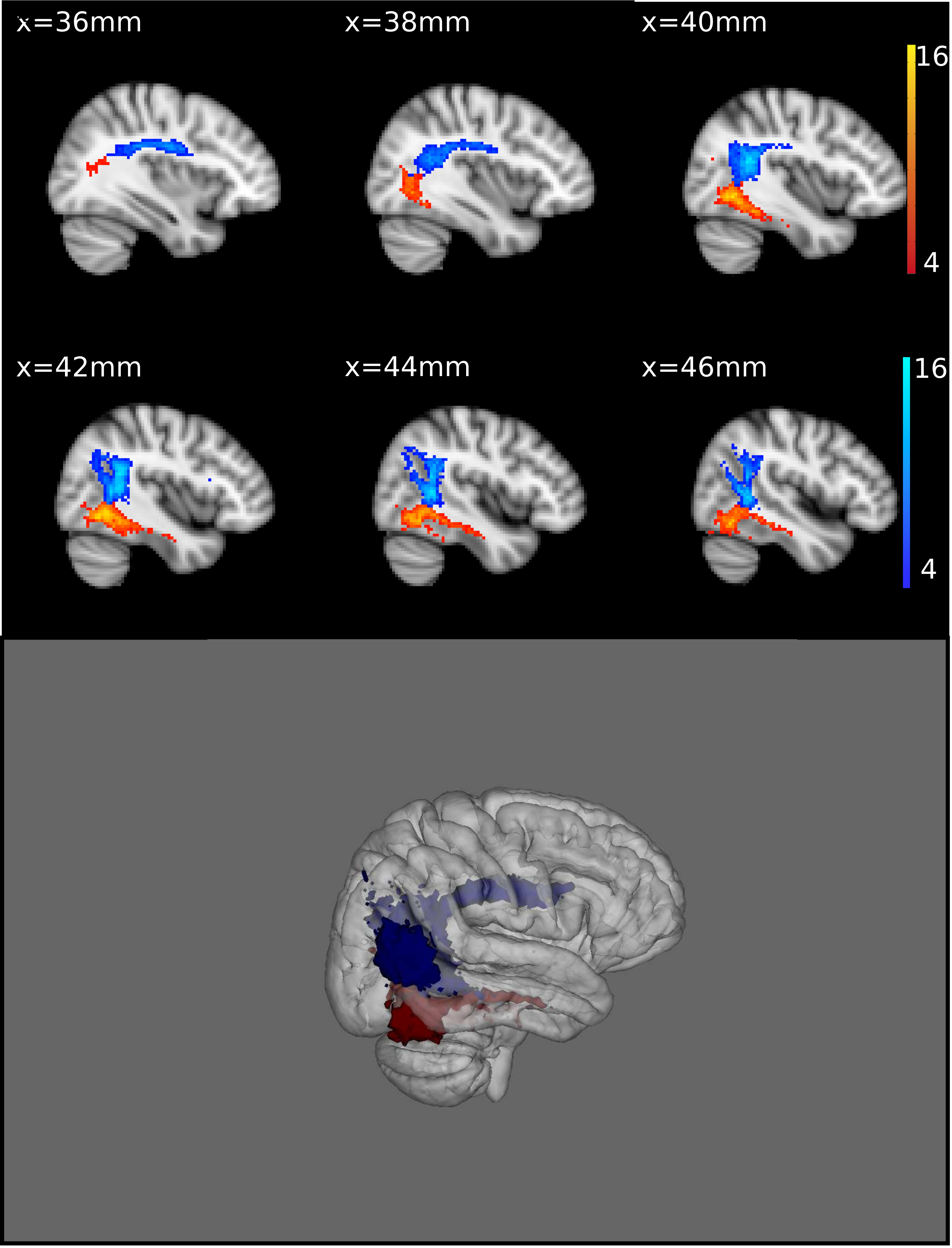
x=36mm
x=38mm
x=40mm
16
4
x=42mm
x=44mm
x=46mm
16
4

Table

Conditions		*d'* mean	±SEM	*C* mean	±SEM	Hit mean	±SEM	False alarm mean	±SEM
Isoluminant	control	3.592	0.211	0.087	0.140	0.9084	0.0229	0.0813	0.0253
	double flash	1.721	0.244	-1.605	0.180	0.9750	0.0108	0.6667	0.0761
Low contrast	control	3.461	0.216	-0.057	0.130	0.9229	0.0210	0.0917	0.0244
	double flash	1.917	0.270	-1.604	0.166	0.9729	0.0115	0.6521	0.0811

Table

	$p<$	No. ofvoxels	X (mm)	Y (mm)	Z (mm)
Right insular WM	0.001	56	36	12	-14
Right infero-temporal WM	0.001	33	45	-60	-8
Left insular WM	0.001	10	-32	21	0

Table

	$p<$	No.of voxels	X (mm)	Y (mm)	Z (mm)
Cerebellar WM	0.001	582	-17	-65	-33
Right parieto-occipital junction	0.001	53	52	-51	9
Right fronto-polar WM	0.001	10	22	56	7
Right superior frontal WM	0.005	4	17	21	51